This is an open access article published under an ACS AuthorChoice License, which permits copying and redistribution of the article or any adaptations for non-commercial purposes.

ACS OMEGA

http://pubs.acs.org/journal/acsodf

Article

Simultaneous Elimination of Dyes and Antibiotic with a Hydrothermally Generated NiAlTi Layered Double Hydroxide Adsorbent

Garima Rathee, Nidhi Singh, and Ramesh Chandra*

Cite This: *ACS Omega* 2020, 5, 2368−2377

Read Online

ACCESS | Metrics & More | Article Recommendations | Supporting Information

ABSTRACT: In this study, a hydrothermal route was used to design a novel NiAlTi layered double hydroxide. The material so-obtained was characterized using various physiochemical techniques such as X-ray diffraction, Fourier transform infrared spectroscopy, thermogravimetric analysis for structural analysis, scanning electron microscopy, transmission electron microscopy for morphological analysis, and so on. The material so-obtained was further applied for wastewater remediation and was found to be an efficient, cost-effective, and reusable adsorbent. Organic contaminants such as dyes and antibiotics were used as pollutants to carry out the removal study. NiAlTi LDH was found to be an excellent adsorbent for the removal of anionic dyes and antibiotics. Excellent performance was shown by NiAlTi LDH at a broad pH range from 4 to 10 for anionic dyes (orange II and methyl orange), but tetracycline removal was predominantly maximum at pH = 9. Further, the kinetic studies also revealed that the adsorption process of both organic contaminants obeyed a pseudo-second-order model. In addition, the Langmuir isotherm adsorption model fitted the experimental results for both types of pollutants very well. The attained maximum adsorption capacity was superb for both organic dyes and antibiotics (1250 mg/g for MO, 2000 mg/g for OII, and 238.09 mg/g for TC). NiAlTi LDH was also capable of simultaneous elimination from a mixture of antibiotics and dyes. Further, NiAlTi LDH also showed outstanding stability and reusability, making it one of the most promising materials for large-scale wastewater remediation contaminated by dyes and antibiotics.

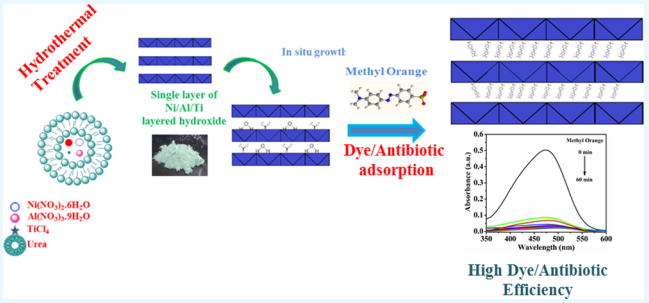

1. INTRODUCTION

The contamination of water resources caused by organic pollutants is a topic of great concern in the last few decades. Among all the sources of pollution, pollution caused by organic dyes and antibiotics in the aquatic system has become a serious threat for human health and the environment.[1] Removal of such water soluble impurities has become very important but is a very tedious job by conventional methods as such impurities easily get transported through rivers and sewage systems.

Among the different water contaminants, organic dyes are especially known for their toxicity even at minute concentrations. Along with their direct effect on health, organic dyes also cause other harmful effects, such as consumption of oxygen molecules, reduction of water transparency, alteration of the oxygen demand, and so on, and thus deteriorate the aquatic life. Anionic as well as cationic dyes are equally toxic, leading to gene mutations and cancer, and if they are allowed to discharge in effluents, serious damage will be caused to human lives.[2]

In the literature, various reports have also shown the occurrence of antibiotics in water bodies, sewage sludge, soil, and sediments.[3] Antibiotics being a special and important group of pharmaceuticals are used worldwide to control infectious diseases, finding importance in animal husbandry and usage in aquaculture industries, which led to a serious concern for their presence in the environment. They are basically categorized into six classes (tetracyclines, macrolides, β-lactams, sulfonamides, fluoroquinolones, and other different antibiotics).[4] Among these antibiotics, tetracycline (TC), which came into application for preserving human health in the 1950s, contains three easily ionizable functional groups, which gets protonated and deprotonated depending upon the pH of the corresponding solutions (a predominantly cationic TC form below pH 3.3, a zwitterionic form within the range 3.3−7.7, and a dominantly anionic form at pH greater than 7.7).[5] Most of the tetracycline on consumption by animals is excreted back to the environment through urine (25−75%) and feces (70−90%), which contaminates surface water and soil. Also, these lead to the growth inhibition of various aquatic

Received: November 6, 2019
Accepted: January 20, 2020
Published: January 30, 2020

© 2020 American Chemical Society

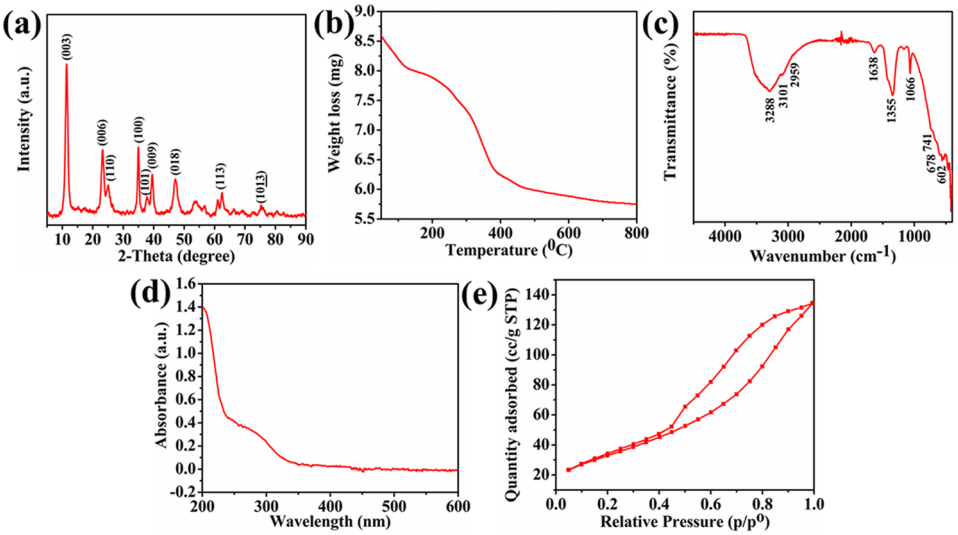

Figure 1. (a) XRD pattern, (b) TGA, (c) FTIR spectrum, (d) UV−vis spectrum, and (e) N_2 adsorption−desorption isotherm of NiAlTi LDH.

species, thus creating antibiotic resistance in the microorganisms and endocrine disruption in the human body.[6]

Thus, it is very important to eliminate organic dye and antibiotic residues from wastewater before they get discharged into nature. Recent studies have shown that among all the well-known conventional methods used for wastewater remediation such as electrochemical processes, membrane filtration processes, photocatalytic processes, oxidation, and ozonation,[7−10] the adsorption process is considered to be the most efficient because of its simplicity, less toxicity, and low cost for the elimination of organic contaminants from effluents. Therefore, various structural modifications and advancements have been made continuously to increase the adsorption capacity of various conventional adsorbents. Among all the reported adsorbents, layered double hydroxides (LDHs) and their modified forms came out as promising adsorbents for water remediation.

LDH, with the general formula $[M_{(1-x)}^{II}M_x^{III}(OH)_2]^{x+}(A^{n-})_{x/n}\cdot mH_2O$ where M^{II} is a divalent metal ion, M^{III} is a trivalent metal ion, and A is the intercalated anion, is one of the most significant inorganic materials.[11] Layered double hydroxides (LDHs) being a porous material have gained huge importance in the field of adsorbents due to their inherent structure, which is capable of capturing various hazardous anionic water pollutants. LDHs generally follow three various mechanisms for controlling such capture of anionic organic/inorganic pollutants, namely, ion-exchange,[12,13] van der Waals forces,[14] and electrostatic attractions.[15] Additionally, H-bonding interactions are also proposed to be formed among the OH groups of LDHs and N- and O-containing groups of adsorbates, but such interactions are found to play a limited role in the adsorption process as only the free hydroxyl groups of the sheets can take part in the interactions with the N-/O-containing groups.[16,17] To our knowledge, various LDHs and their modified forms have been designed by various research groups and implemented for water remediation, but none of them has shown outstanding results for simultaneous removal of various organic contaminants (such as dyes and antibiotics).[18]

Herein, our group has designed a novel LDH material by using a hydrothermal method. The resulting material was characterized by various techniques, such as X-ray diffraction (XRD), thermogravimetric analysis (TGA), Fourier transform infrared spectroscopy (FTIR), scanning electron microscopy (SEM), high-resolution transmission electron microscopy (HRTEM), UV−vis spectroscopy, and N_2 adsorption−desorption techniques. In this study, we have used the designed adsorbent for the removal of anionic organic water contaminants (methyl orange (MO), orange II (OII), and tetracycline (TC)). Furthermore, the influences of the various parameters such as solution pH, adsorbent dosage, contact time, and initial dye/antibiotic concentrations were also evaluated. Additionally, the adsorption kinetics and adsorption isotherms were analyzed for both organic contaminants using theoretical models. Further, the adsorbent was also implemented to evaluate the simultaneous removal of both the dye and antibiotic from the mixture of equal concentrations of both contaminants. The reusability of the adsorbent was also tested.

2. RESULTS AND DISCUSSION

2.1. Characterization of NiAlTi LDH. The XRD (X-ray diffraction) pattern of NiAlTi LDH is illustrated in Figure 1a. The recorded diffraction peaks are found to be very compatible with previously reported data.[19,43] The (00L) series diffraction peaks ((003), (006), (009)) are observed at 11.44, 23.25, and 39.59°, respectively, indicating the existence of a lamellar structure with the intercalation of carbonate ions and water molecules within the lattice of the LDH. The *d* spacings with respect to reflection planes (003) and (110) were 0.773 nm (2θ = 11.438°) and 0.354 nm (2θ = 25.077°), respectively. As the obtained basal spacing can be easily correlated with the previously synthesized Ti-assimilated LDHs, the usual outcome could be the formation of a pattern by the interlayered CO_3^{2-} anions and H_2O molecules. The existence of the anatase phase of TiO_2 in the designed LDH is verified by the presence of diffraction planes (110) and (101) at 2θ = 25.08 and 37.70°, respectively. The existence of sharp, intense, and narrow peaks is attributed to the great crystallinity of the synthesized NiAlTi LDH material. Moreover, the presence of peaks at 2θ values of 35.00, 47.09, 62.48, and 75.18° shows the existence of other reflections, (100), (018), (113), and (10$\underline{13}$), respectively, indicating the typical LDH material with interlayered carbonate ions and water molecules. Various XRD parameters are reported in Table S1.

https://dx.doi.org/10.1021/acsomega.9b03785
ACS Omega 2020, 5, 2368−2377

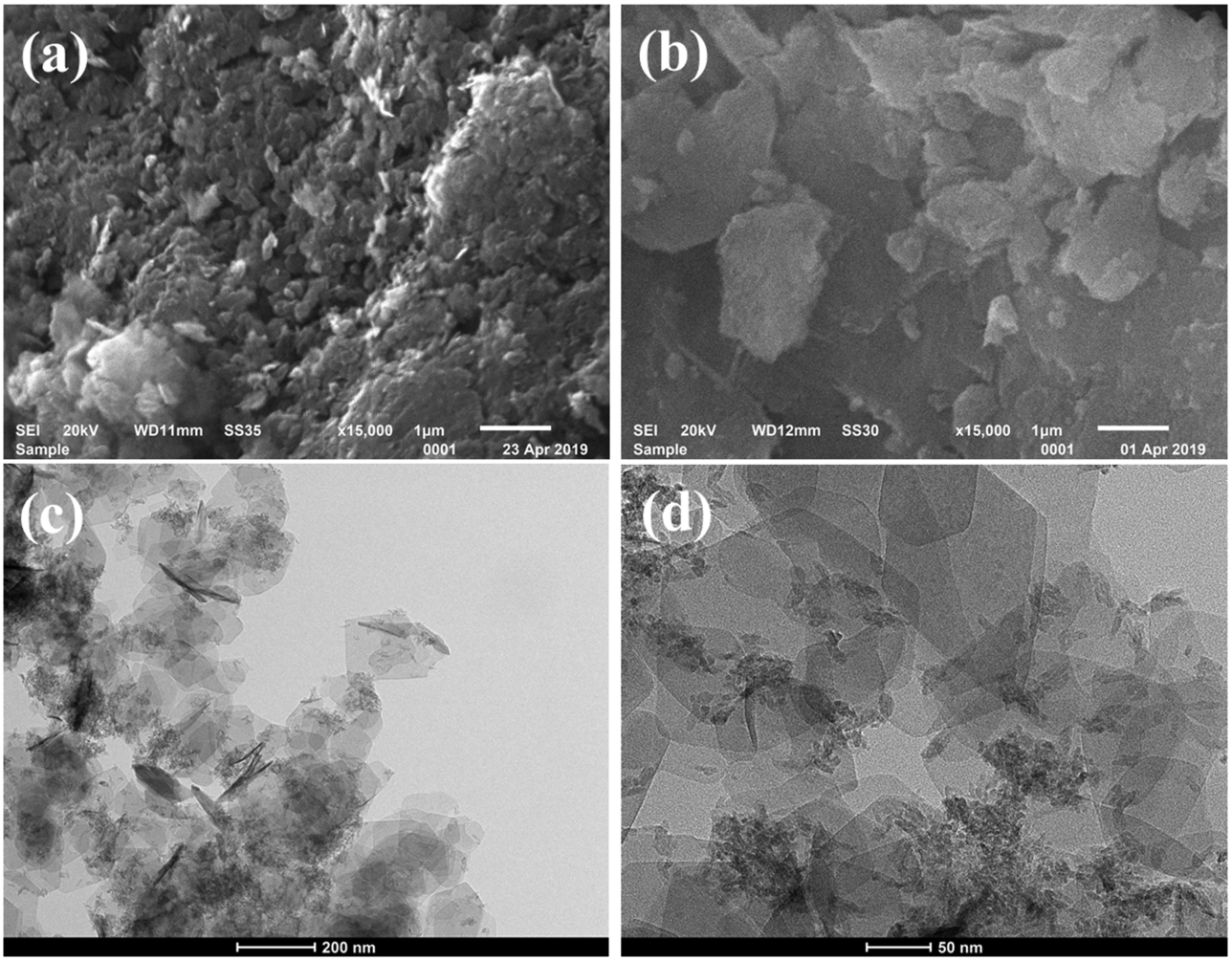

Figure 2. (a, b) SEM and (c, d) TEM images of NiAlTi LDH.

The TGA curve of the designed LDH material mainly exhibits two degradation steps (Figure 1b). The first degradation step is observed in the temperature range of 50−200 °C attributed to the elimination of the physisorbed interlayered H_2O molecules. The second degradation, observed at 250−400 °C, is attributed to the brucite layer dehydration and interlayered carbonate ion decomposition.[19]

The FTIR spectra of the synthesized LDH material, depicted in Figure 1c, exhibited all the characteristic frequencies related to the carbonated LDHs. The absorption band present at 3288 cm^{-1} could be ascribed to the stretching vibration due to the water molecules present on the surface and to the interlayered ones within the LDH and hydroxyl group. This stretching vibration occurs at lower wavenumbers as compared to that of free water (3600 cm^{-1}), which clearly indicates the presence of H_2O molecules placed between the layers of synthesized NiAlTi LDH. The existence of the H bond between the interlayered water molecules and CO_3^{2-} ions is confirmed due to the presence of shoulders at 3101 and 2959 cm^{-1}. The absorption band at 1638 cm^{-1} could be allotted to the bending mode of H_2O molecules. The vibrational bands at 1355, 1066, and 741 cm^{-1} could be due to the existence of CO_3^{2-} ions. The presence of bands at 678 and 602 cm^{-1} could be attributed to M−OH and M−O bonds in synthesized NiAlTi LDH. Thus, the FTIR analysis combined with other studies leads to the confirmation of the existence of carbonate and water molecules within the interlayer sheets of LDH.[20] In the UV−vis spectra of NiAlTi LDH (Figure 1d), an optical absorption band is observed around 200−300 nm, which might be due to the ligand to metal charge transfer in the octahedra of LDH. Further, the presence of a strong adsorption band within the 250−450 nm range can be attributed to the coordination of the metal with the intercalated carbonate anions of the synthesized LDH material.[19]

The nitrogen adsorption−desorption study at 77 K clearly indicates characteristic properties depicted by mesoporous materials. The isotherm clearly indicates that the condensed N_2 in the pores followed distinct paths with the release of reduced pressure. NiAlTi LDH followed a type-IV isotherm along with a broad H3-type hysteresis loop (at $P/P_0 > 0.4$) (Figure 1e). The observed BET surface area, pore volume, and pore diameter of LDH are 121.845 mg^2/g, 0.212 cc/g, and 3.82 nm, respectively.[19]

SEM images of NiAlTi LDH are shown in Figure 2a,b. Platelet-like structures are observed in SEM images. The overlapping of these platelets results in the formation of irregular particle sizes. TEM images of NiAlTi LDH are shown in Figure 2c,d. The TEM images clearly indicate the non-uniform and irregular sheet-like morphology of NiAlTi LDH.[19] The EDAX analysis of NiAlTi LDH, depicted in Figure S1, indicates that the average elemental percentages of Ni, Al, and

https://dx.doi.org/10.1021/acsomega.9b03785
ACS Omega 2020, 5, 2368−2377

Ti are 22.32, 11.75 and 8.78%, respectively, and the approximate ratio of elements is Ni/Al/Ti = 2:1:1.

2.2. Adsorption Study. NiAlTi LDH being a porous layered material with additional properties of high BET surface area was found to be a tremendous adsorbent for water remediation. The adsorption process was evaluated by means of UV−vis spectroscopy by assessing the variations in the characteristic peaks of different organic pollutants. While accessing the data, a gradual decrease in the characteristic peaks was observed with the progression of the reaction, signifying a decrease in the concentrations of organic contaminants (Figure S2). In the initial stage, the dye removal efficiency of NiAlTi LDH was evaluated for a wide range of dyes (methyl orange (MO), orange II (OII), methylene blue (MB), and rhodamine B (RB)). It was observed from the data that both the anionic dyes were almost completely eliminated (MO = 96.71% and OII = 100%) from the synthetic wastewater solutions as compared to the partial removal of the cationic dyes, (MB = 5% and RB = 14%) depicted in Figure 3 (reaction conditions: adsorbent amount, 4 mg; volume of dye sample, 10 mL; concentration of initial dye sample, 20 mg/L; temperature, 25 ° C; and time, 60 min). Such behavior of NiAlTi LDH is observed because of the electrostatic attraction between the negatively charged anionic dyes and positively charged LDH host layers, which results in the complete adsorption of MO and OII, whereas less adsorption of MB and RB was observed due to electrostatic repulsion between the positively charged LDH layers and cationic dyes.[21] Therefore, NiAlTi LDH is highly effective for the elimination of anionic over cationic dyes, so the further studies were carried out only for anionic dyes (MO and OII).

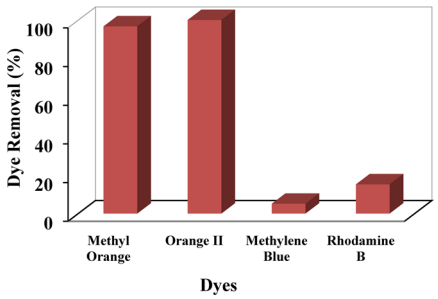

Figure 3. Dye removal efficiency of NiAlTi LDH for various dyes.

Primarily, the effect of pH variation on the dye removal (%) efficiency of the synthesized adsorbent was evaluated (reaction conditions: adsorbent amount, 4 mg; volume of dye sample, 10 mL; concentration of initial dye sample, 20 mg/L; temperature, 25 ° C; and time, 60 min). From the experimental results, it was observed that both dyes (MO and OII) illustrated analogous adsorption behavior at a selected pH range (Figure 4a). Results clearly displayed that the adsorption capacity slightly increased as the pH of the reaction mixture increases from 4 to 8−9 and greatly decreased as the pH further increases toward highly basic conditions, that is, 12. According to the results, the maximum adsorption capacity was obtained at pH 8 and 9, that is, 96.70% for MO and 100% removal for OII (approximately equal cleaning efficiency for both pH values). On lowering the pH toward the acidic side, we brought the adsorbent more toward the dissolution process, which affected the availability of active sites and further decreased the removal efficiency from 96.70% (pH = 8) to 94.4% (pH = 4) when MO was used as the adsorbate and 100% (pH = 8) to 96.04% (pH = 4) when OII was employed. On increasing the pH toward the basic side, the negative charge on the adsorbent surface also increases simultaneously, resulting in higher electrostatic repulsion among the adsorbent surface and anionic dye molecules.[22] Hence, pH = 8 was carefully chosen as the optimum pH for further evaluation.

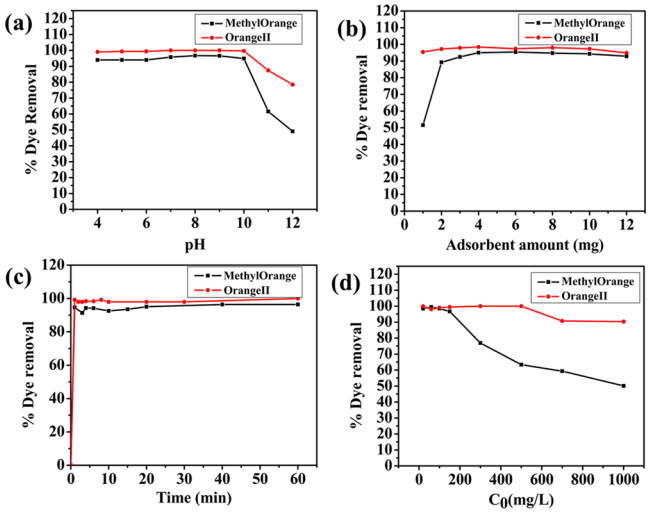

Figure 4. Effects of (a) pH, (b) adsorbent amount, (c) contact time, and (d) initial antibiotic concentration on the adsorption process of methyl orange and orange II over NiAlTi LDH.

Further, the optimum amount of adsorbent was investigated with 20 mg/L initial dye sample with varied adsorbent dosages (varying from 0.1 to 1.2 g/L) at pH = 8 (depicted in Figure 4b). From the recorded data, it was observed that the dye removal was efficient and rapid with complete removal of MO and OII within several minutes. With the increasing amount of adsorbent, the dye removal efficiency also rises and became almost constant after a certain amount was added when maximum adsorption efficiency was attained. The maximum adsorption efficiency (98.48% (MO) and 100% (OII)) was attained with 0.4 g/L amount of NiAlTi LDH. Hence, 0.4 g/L adsorbent dosage was selected as the optimum dosage for dye removal. Also, further studies were carried out to estimate the equilibrium time for the removal of dyes by determining the effects of time on MO and OII removal, and the results are depicted in Figure 4c (reaction conditions: adsorbent amount, 4 mg; volume of dye sample, 10 mL; concentration of initial dye sample, 20 mg/L; temperature, 25 ° C; time, 1 h; and pH = 8). Equilibrium was achieved within 20 min for MO and 10 min for complete adsorption of OII from wastewater solution.

Also, the effect of initial MO and OII concentrations on the adsorption process was studied with 0.4 g/L adsorbent amount and is depicted in Figure 4d. The dye removal efficiency (%) for MO remained almost the same when the initial MO concentration varied from 20 to 150 mg/L, but on further increasing the concentration up to 1000 mg/L, the removal efficiency declined from 96.67% (150 mg/L) to 50.14% (1000 mg/L). A similar falling behavior was detected for the OII dye, declining from 99% (at 500 mg/L) to 90.3% (1000 mg/L). Such a decline in removal efficiency is obtained because of the presence of a fixed amount of adsorption sites in NiAlTi LDH for a certain adsorbent dosage. After filling of these adsorption sites, due to the absence of free active sites, the dye removal efficiency fell with increasing concentration for both cases.

https://dx.doi.org/10.1021/acsomega.9b03785
ACS Omega 2020, 5, 2368−2377

Additionally, NiAlTi LDH performance for the adsorptive elimination of antibiotics from pharmaceutical wastewater was also evaluated. For the adsorption of antibiotics, the pH of the solution is the key factor for controlling the adsorption process. The solution pH has a direct impact on the charge of the layers of the adsorbent and the molecular structure of the antibiotic. For this study, the antibiotic tetracycline (TC) was employed. Initially, the pH optimization was carried out with 60 mg/L TC solution and is illustrated in Figure 5a. The results clearly

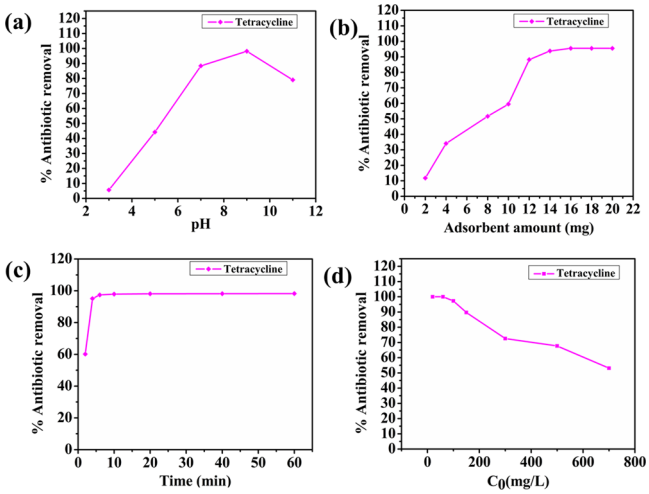

Figure 5. Effects of (a) pH, (b) adsorbent amount, (c) contact time, and (d) initial antibiotic concentration on the adsorption process of tetracycline over NiAlTi LDH.

displayed an increasing slope with the increase in pH clearly pointing toward the enhancement in the antibiotic removal efficiency of the adsorbent. Maximum adsorption (98.164%) was attained at pH = 9, beyond which the removal efficiency decreased with increasing pH. A low adsorption capacity was observed at low pH values because of the complete protonation of the molecule with a positive overall charge of the predominant cationic tetracycline form due to which the electrostatic repulsion occurs between the positive charge of cationic form of TC and layers of the host material. With the increase of pH, deprotonation comes into play, leading to the formation of anionic TC, which gets intercalated within the LDH lattice, resulting in higher antibiotic removal. However, at greater pH values, electrostatic repulsion between the anionic form of TC and increased negative charge on the surface of the adsorbent plays a key role in the decrease in the adsorptive efficiency of NiAlTi LDH.

Further, the optimum amount of NiAlTi LDH for TC removal was determined with 60 mg/L TC solution at pH = 9. Figure 5b depicts the influence of adsorbent dosage on the elimination of TC from the TC synthetic sample. From the experimental data, it was evaluated that the maximum adsorption was achieved with a 1.6 g/L (16 mg of adsorbent for 60 mg/L TC sample (10 mL)) adsorbent dosage. Time variation was further evaluated to determine the equilibrium time of the adsorption process and is depicted in Figure 5c. The rate of adsorption was found to be very fast and achieved equilibrium 20 min from the start of the reaction. Additionally, the effect of variation in the concentration of the initial TC sample is depicted in Figure 5d. At lower concentrations up to 60 mg/L TC sample, the adsorbent was found to be highly efficient with 100% elimination of TC. On further increasing the concentration, the removal efficiency decreased and reduced to approximately half, that is, 53.08% at 700 mg/L initial TC concentration. Such behavior is obtained because the adsorbent consists of a fixed number of active sites and, at higher concentrations, when these sites are completely filled, the TC adsorption decreases with the rise in the concentration.

2.3. Kinetics Study. The kinetics experimental data was fitted to kinetic models (pseudo-first-order and pseudo-second-order) to study the adsorption behavior of NiAlTi LDH toward anionic dyes and antibiotics. According to the pseudo-first-order kinetic model (eq 1)

$$\log(q_e - q_t) = \log(q_e) - \frac{k_1}{2.303}t \quad (1)$$

where q_e and q_t represents the amount of MO, OII, and TC adsorbed at equilibrium time and at time t, respectively, and k_1 denotes the reaction rate constant. The slope of the linear plot between $\log(q_e - q_t)$ and time t gives us k_1. The pseudo-first-order kinetic plots are shown in Figure 6a,b for MO and OII and in Figure 8a for TC.

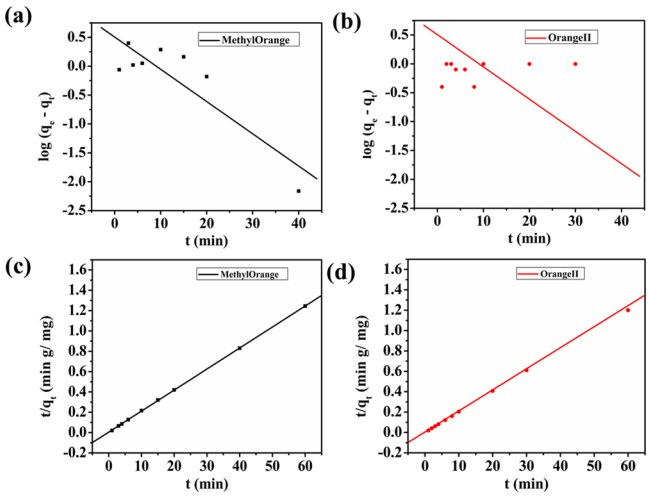

Figure 6. Pseudo-first-order kinetics plots for (a) methyl orange and (b) orange II and pseudo-second-order kinetics plots for (c) methyl orange and (d) orange II.

According to the pseudo-second-order kinetic model (eq 2), the adsorption rate is controlled by the chemical adsorption. The pseudo-second-order equation is depicted as

$$\frac{t}{q_t} = \frac{1}{k_2 q_e^2} - \frac{1}{q_e}t \quad (2)$$

where k_2 is the second-order adsorption rate constant and q_e and R^2 are calculated from the constants (slope and intercept) obtained from the linear plot between t/q_t and t. Pseudo-second-order plots of MO and OII are illustrated in Figure 6c,d, and that of TC is illustrated in Figure 8b. All the constants and R^2 values are summarized in Table 1. It could be easily stated from the results that adsorption of MO, OII, and TC onto NiAlTi LDH was found to follow the pseudo-second-order kinetic model based on the R^2 values, which were almost close to unity in all the three cases.

2.4. Isotherm Study. Langmuir and Freundlich equations were used to evaluate the adsorption isotherms. According to the Langmuir isotherm model, the adsorption energy is assumed to be constant. It is also assumed that the molecules

https://dx.doi.org/10.1021/acsomega.9b03785
ACS Omega 2020, 5, 2368−2377

Table 1. Pseudo-First-Order and Pseudo-Second-Order Parameters for MO, OII, and TC

	pseudo-first order			pseudo-second order		
adsorbates	q_e (mg/g)	k_1 (min^{-1})	R^2	q_e (mg/g)	k_2 (g/mg min)	R^2
MO	3.2084	0.1287	0.77	48.30	0.0912	0.999
OII	1.3449	0.0145	0.13	49.02	1.04	1
TC	1.755	0.1382	0.649	37.174	0.0664	0.999

of the adsorbate do not hold any kind of interactions during the adsorption.[23] The Langmuir isotherm linear equation is denoted as

$$\frac{C_e}{q_e} = \frac{1}{q_m b} + \frac{C_e}{q_m} \quad (3)$$

where C_e (mg/L) represents the equilibrium concentration of the dye or antibiotic used and q_e (mg/g) represents the amount of dye/antibiotic adsorbed per unit adsorbent. q_m (mg/g) and b (L/mg) are the Langmuir constants obtained from the slope and intercept of the plot between C_e/q_e and C_e, respectively. Both the constants are interrelated with the adsorption rate and capacity. One of the Langmuir equation's essential characteristics can be expressed as dimensionless R_L (separation factor), which is denoted by

$$R_L = \frac{1}{1 + bC_0} \quad (4)$$

where C_0 represents the initial dye/ antibiotic concentration. From the R_L value, we can detect whether the adsorption is favorable ($0 < R_L < 1$), unfavorable ($R_L > 1$), linear ($R_L = 1$), or irreversible ($R_L = 0$). The Freundlich model that is based on the assumption that non-uniform distribution of heat occurs over heterogeneous surfaces is given by

$$\log q_e = \log K_f + \frac{1}{n}\log C_e \quad (5)$$

where q_e and C_e have their usual meanings. K_f and n represents Freundlich constants, which are basically related to both adsorption capacity and intensity, respectively. Both the constants (K_f and n) are obtained from the intercept and slope of the linear plot between log q_e and log C_e, respectively. The model fitting for MO and OII is depicted in Figure 7 and for TC in Figure 8c,d. All the parameters obtained from the isotherm studies are reported in Table 2. From the data depicted in Table 2, it can be stated that the Langmuir model gave greater correlation coefficient values (R^2) for all the three contaminants, which clearly indicates that the adsorption over the adsorbent is a monolayer. From the obtained R_L values depicted in Figure S3, which lie completely between 0 and 1 for all the contaminants, it can be concluded that the adsorption process was favorable and consisted of homogeneous patches. On comparison of the obtained maximum adsorption capacities for MO, OII, and TC with previously reported adsorbents, it could be easily stated that our material NiAlTi LDH showed greater adsorption capacity for both types of pollutants (dyes and antibiotics) among all the previously reported adsorbents (Table 3).[18,22,25−42] Therefore, our material exhibits excellent adsorption properties for different types of pollutants and could be considered as a potential adsorbent for the elimination of various organic contaminants from waste water systems.

The mechanism behind the adsorption of MO, OII, and TC over synthesized NiAlTi LDH was investigated using FTIR

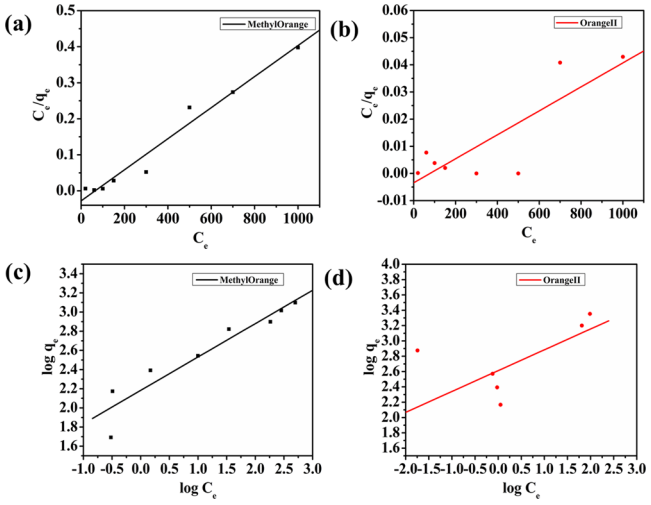

Figure 7. Langmuir plots of the isotherms for (a) methyl orange and (b) orange II and Freundlich plot of isotherms for (c) methyl orange and (d) orange II.

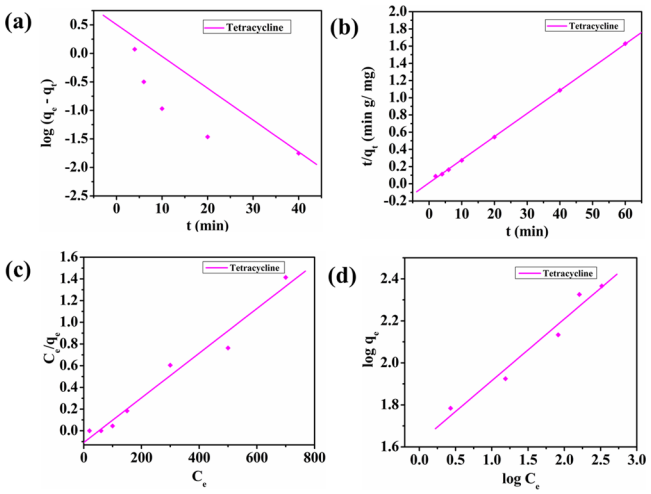

Figure 8. (a) Pseudo-first-order kinetic plot, (b) pseudo-second-order kinetic plot, (c) Langmuir plot of isotherm, and (d) Freundlich plot of isotherm for tetracycline.

spectroscopy. FTIR spectra of LDH before and after the adsorption of contaminants are depicted in Figure 9a. The intercalation of MO, OII, and TC into NiAlTi LDH can be confirmed by the formation of new vibrational bands occurring in the region of 1300−1000 cm^{-1}. In the case of intercalation of MO, these new vibrational bands at 1029 and 1119 cm^{-1} could be attributed to the vibrations due to the $-SO_3^-$ group of MO and the 1,4-substituted benzene ring. The presence of new bands at 1166 and 1606 cm^{-1} could be due to the stretching vibrations of C−N and C═C bonds of MO molecules, respectively. Similar bands were observed in the case of the OII dye. In the case of tetracycline adsorption, new

https://dx.doi.org/10.1021/acsomega.9b03785
ACS Omega 2020, 5, 2368−2377

Table 2. Langmuir and Freundlich Parameters for MO, OII, and TC

	Langmuir model			Freundlich model		
adsorbates	q_m (mg/g)	b (L/mg)	R^2	K_f (mg/g)(L/mg)$^{1/n}$	n	R^2
MO	1250	0.039	0.964	152.47	2.87	0.89
OII	2000	0.2	0.946	470.54	3.67	0.47
TC	238.09	0.0579	0.97	26.39	2.538	0.85

Table 3. Comparison of Maximum Adsorption Capacities of NiAlTi LDH for MO, OII, and TC with Different Adsorbents

adsorbents	adsorbates	q_{max} (mg g^{-1})	ref
banana peel	MO	21.0	25
orange peel	MO	20.0	25
deoiled soya	MO	16.66	26
bottom ash	MO	3.62	26
MgFe-LDO	MO	104.27	26
MgAl-LDO	MO	134.27	27
ZnAl-LDO	MO	181.9	28
MgAl-LDH	MO	169.11	29
Fe_3O_4/ZnCr-LDH	MO	535.5	22
Au/ZnAl-LDO	MO	627.51	30
NiAlTi LDH	MO	1250	present study
Mg/Al LDH	OII	224	31
calcined Mg/Al LDH	OII	602	31
Mg/Al-NDH-NO_3	OII	947.1	32
LDHs of compositions, Mg/Al, Cu/Al, Co/Al, Mg/Cu/Al, Co/Cu/Al, and Mg/Co/Al	OII	59.2–129.8	33
acid and base-functionalized titanosilicate	OII	98 and 49	34
activated carbon	OII	329	35
mesoporous carbon CMK-3	OII	385	35
ammonia-tailored CMK-3	OII	596	35
zirconium-based chitosan microcomposite adsorbent	OII	926	36
Mg/Al HT calcined	OII	634.4	37
HT macro calcined	OII	1521.2	37
LDH/PEG	OII	625	38
NiAlTi LDH	OII	2000	present study
activated sludge	TC	72	39
montmorillonite	TC	54	40
palygorskite	TC	99	41
rectorite	TC	140	42
CSLDO400	TC	195.31	18
NiAlTi LDH	TC	238.09	present study

vibrational bands at 1356 and 1616 cm^{-1}, which are the main vibrational bands of TC, confirm the adsorption of TC over the surface. In all the three cases, disappearance of the vibrational band at 1355 cm^{-1} as compared to the raw LDH FTIR spectra reveals the elimination of carbonate ions and intercalation of dye/antibiotic molecules, which leads to the conclusion that the mechanism behind such adsorption could be the ion exchange mechanism (Figure 9b).[24]

The exhausted NiAlTi LDH was regenerated and its recyclability was carried out for five consecutive cycles. The removal efficiency of regenerated NiAlTi LDH for every consecutive cycle is depicted in Figure 10. From the bar results, it could be clearly inferred that even after the fifth cycle,

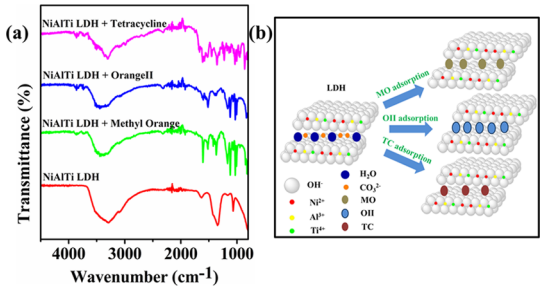

Figure 9. (a) FTIR spectra of NiAlTi LDH, methyl orange-adsorbed NiAlTi LDH, orange II-adsorbed NiAlTi LDH, and tetracycline-adsorbed NiAlTi LDH. (b) Schematic illustration of MO, OII, and TC adsorption over NiAlTi LDH.

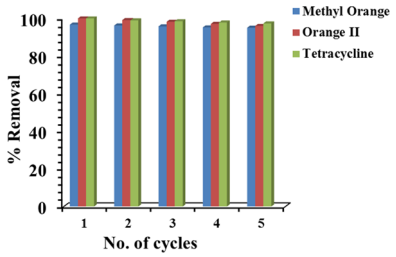

Figure 10. Recyclability of NiAlTi LDH for the removal of various organic contaminants (MO, OII, and TC).

the efficiency of NiAlTi LDH was found to be >95% for all the three contaminants. Thus, it can be concluded from the recyclability results that NiAlTi LDH is easily recoverable, can be easily regenerated, and is highly stable and highly efficient for eliminating organic contaminants from water. The cleaning efficiency of NiAlTi LDH was also evaluated for the mixture of a dye (MO) and an antibiotic (TC) (reaction conditions: adsorbent dosage = 4 mg, MO concentration = 20 mg/L, TC concentration = 20 mg/L, volume of solution = 10 mL, temperature = 25 ° C, pH = 9, time = 60 min). From the results, NiAlTi LDH was found to be an excellent adsorbent to eliminate both the contaminants from the mixture with a great removal efficiency of 99% for MO and 98% for TC. Thus, NiAlTi LDH is an excellent adsorbent for simultaneous removal of MO and TC.

3. CONCLUSIONS

In this study, we have successfully designed and synthesized a novel and highly pure NiAlTi LDH by using a hydrothermal method. The synthesized material was implemented for the elimination of organic contaminants (dyes and antibiotics) from waste solutions. The as-prepared NiAlTi LDH with a high surface area resulted in excellent elimination of organic water contaminants. The observed adsorption equilibrium times are 20 min for MO, 10 min for OII, and 20 min for TC. The attained maximum adsorption capacity was superb for both organic dyes and antibiotics (1250 mg/g for MO, 2000 mg/g for OII, and 238.09 mg/g for TC). The active pH and

https://dx.doi.org/10.1021/acsomega.9b03785
ACS Omega 2020, 5, 2368−2377

NiAlTi LDH dosage for complete removal of dyes were 8 and 0.4 g/L (for 20 ppm concentrated dye solution) and those for complete elimination of antibiotic (TC) were 9 and 1.6 g/L (for 60 ppm concentrated antibiotic solution), respectively. Both pollutants were found to be easily correlated with the pseudo-second-order kinetic model for the adsorption process. The Langmuir isotherm adsorption model fitted the experimental results for both types of pollutants very well. Also, NiAlTi LDH was capable of simultaneous elimination of antibiotics and dyes. Further, NiAlTi LDH also showed outstanding stability and reusability, making it one of the most promising materials for large-scale wastewater remediation contaminated by dyes and antibiotics.

4. EXPERIMENTAL SECTION

4.1. Materials. All the chemicals used in this study were commercially available and used as supplied without further purification. Aluminum nitrate nonahydrate, methyl orange, and orange II were purchased from Sigma Aldrich, nickel nitrate hexahydrate from THOMAS BAKER, titanium tetrachloride from LOBA CHEMIA, and tetracycline hydrochloride from SRL. All other chemicals were procured from commercial suppliers.

4.2. Synthesis of NiAlTi Layered Double Hydroxide. NiAlTi LDH was synthesized by a hydrothermal route. $Ni(NO_3)_2{\cdot}6H_2O$ (5.49 g), 3.540 g of $Al(NO_3)_2{\cdot}9H_2O$, 0.6 mL of $TiCl_4$, and 1.5 g of urea (used as a template, which on hydrolysis during hydrothermal treatment gives carbonate and ammonium ions) were dissolved in deionized water. The mixture was transferred to an autoclave and aged hydrothermally for 40 h at 160 °C. The product so-obtained was extracted, washed with deionized water, and dried for 24 h at 60 °C.[43]

4.3. Characterization. The synthesized NiAlTi LDH was characterized for its phase purity, crystal structure, morphology, and specific surface area. The LDH morphology was examined by using a JEOL JSM 6610 SEM with an accelerating voltage of 30 kV and a TECNAI 200 kV HRTEM (Fei, Electron Optics). The BET specific surface area of LDH was examined by the Brunauer–Emmett–Teller (BET) method on an Autosorb iQ Station 1 (Quantachrome Instruments). The FTIR spectrum was investigated on an IRAffinity-1S FTIR (Shimadzu). The phase purity and crystallinity were evaluated using an X-ray diffractometer (model no. D8 DISCOVER). Thermogravimetric analysis (TGA) was determined using a LINSEIS L40/2052. Adsorption studies were estimated using a Thermo Scientific Evolution 300 UV–vis spectrometer.

4.4. Adsorption Experiments. The dye and antibiotic adsorption over NiAlTi LDH was evaluated as batch experiments. Effects of certain parameters—time, pH, adsorbent amount, and initial dye/antibiotic concentrations—were evaluated. For the dye adsorption experiments, initially, the effect of pH variation was studied within a pH range (4–12) and the optimum pH of the initial dye solution was adjusted via 0.1 N HCl and 0.1 N NaOH. Then, the effect of adsorbent amount was studied within the range of 0.1–1.2 g/L. Further, a kinetics study was conducted with 0.4 g/L adsorbent concentration and 20 ppm initial dye concentration at the optimum pH of the solution. Then, the adsorption isotherms were also evaluated with initial dye concentrations varying within the range of 10–1000 mg/L. Similarly, an antibiotic adsorption study was also conducted. Additionally, the recyclability of the adsorbent was also evaluated for the dyes and antibiotics by the method described below. The adsorbent was recovered by centrifugation after the reaction has attained equilibrium and washed with deionized water to remove leftover dye/antibiotic molecules. The adsorbent was further allowed to stir in 30 mL of ethanol for 6 h. Finally, the adsorbent was separated, washed with decarbonated water, dried, and applied for the next adsorption cycle. The reusability was studied for five cycles. The residual dye/antibiotic concentrations were estimated by using a UV–vis spectroscope (Thermo Scientific Evolution 300), and the adsorption capacity was evaluated using the conventional equation

$$\text{adsorption capacity } (q_e) = \frac{C_0 - C_e}{m} V \tag{6}$$

where C_0 represents the initial dye/antibiotic concentration (mg/L), C_e represents the equilibrium dye/antibiotic concentration (mg/L), m represents the mass of the LDH adsorbent used (g), and V represents the volume of dye/antibiotic solution in liters.

■ ASSOCIATED CONTENT

Supporting Information

The Supporting Information is available free of charge at https://pubs.acs.org/doi/10.1021/acsomega.9b03785.

XRD parameters, EDAX analysis of NiAlTi LDH, UV–visible spectra of time-dependent adsorption, R_L versus C_0 plot, and structures and properties of the adsorbates tested (PDF)

■ AUTHOR INFORMATION

Corresponding Author

Ramesh Chandra − *Drug Discovery & Development Laboratory, Department of Chemistry and Dr. B. R. Ambedkar Centre for Biomedical Research, University of Delhi, Delhi, India*; Email: acbrdu@hotmail.com

Authors

Garima Rathee − *Drug Discovery & Development Laboratory, Department of Chemistry, University of Delhi, Delhi, India*; orcid.org/0000-0001-6825-3563

Nidhi Singh − *Drug Discovery & Development Laboratory, Department of Chemistry, University of Delhi, Delhi, India*

Complete contact information is available at: https://pubs.acs.org/10.1021/acsomega.9b03785

Notes

The authors declare no competing financial interest.

■ ACKNOWLEDGMENTS

G.R. and R.C. are greatly thankful to the University of Delhi for providing financial support. We are also grateful to DST-SERB (EMR/2016/2976) for providing the financial assistance.

■ REFERENCES

(1) Piccin, J. S.; Gomes, C. S.; Feris, L. A.; Gutterres, M. Kinetics and isotherms of leather dye adsorption by tannery solid waste. *Chem. Eng. J.* **2012**, *183*, 30–38.

(2) Yan, S. C.; Li, Z. S.; Zou, Z. G. Photodegradation of Rhodamine B and Methyl Orange over Boron–Doped g-C_3N_4 under Visible Light Irradiation. *Langmuir* **2010**, *26*, 3894–3901.

(3) Arpin-Pont, L.; Bueno, M. J. M.; Gomez, E.; Fenet, H. Occurrence of PPCPs in the marine environment: a review. *Environ. Sci. Pollut. Res.* **2016**, *23*, 4978−4991.
(4) Michael, I.; Rizzo, L.; McArdell, C. S.; Manaia, C. M.; Merlin, C.; Schwartz, T.; Dagot, C.; Fatta-Kassinos, D. Urban wastewater treatment plants as hotspots for the release of antibiotics in the environment: a review. *Water Res.* **2013**, *47*, 957−995.
(5) Premarathna, K. S. D.; Rajapaksha, A. U.; Adassoriya, N.; Sarkar, B.; Sirimuthu, N. M. S.; Cooray, A.; Ok, Y. S.; Vithanage, M. Clay-biochar composites for sorptive removal of tetracycline antibiotic in aqueous media. *J. Environ. Manage.* **2019**, *238*, 315−322.
(6) Halling-Sørensen, B. Algal toxicity of antibacterial agents used in intensive farming. *Chemosphere* **2000**, *40*, 731−739.
(7) Košutić, K.; Dolar, D.; Ašperger, D.; Kunst, B. Removal of antibiotics from a model wastewater by RO/NF membranes. *Sep. Purif. Technol.* **2007**, *53*, 244−249.
(8) Koyuncu, I.; Arikan, O. A.; Wiesner, M. R.; Rice, C. Removal of hormones and antibiotics by nanofiltration membranes. *J. Membr. Sci.* **2008**, *309*, 94−101.
(9) Chen, F.; Yang, X.; Mak, H. K. C.; Chan, D. W. T. Photocatalytic oxidation for antimicrobial control in built environment: a brief literature overview. *Build. Environ.* **2010**, *45*, 1747−1754.
(10) Lee, H.; Lee, E.; Lee, C.-H.; Lee, K. Degradation of chlorotetracycline and bacterial disinfection in livestock wastewater by ozone-based advanced oxidation. *J. Ind. Eng. Chem.* **2011**, *17*, 468−473.
(11) Pourfaraj, R.; Fatemi, S. J.; Kazemi, S. Y.; Biparva, P. Synthesis of hexagonal mesoporous MgAl LDH nanoplatelets adsorbent for the effective adsorption of Brilliant Yellow. *J. Colloid Interface Sci.* **2017**, *508*, 65−74.
(12) Setti, N. D.; Jouini, N.; Derriche, Z. Sorption Study of an Anionic Dye-Benzopurpurine 4B-on Calcined and Uncalcined Mg-Al Layered Double Hydroxides. *J. Phys. Chem. Solids* **2010**, *71*, 556−559.
(13) Zaghouane-Boudiaf, H.; Boutahala, M.; Arab, L. Removal of Methyl Orange from Aqueous Solution by Uncalcined and Calcined MgNiAl Layered Double Hydroxides (LDHs). *Chem. Eng. J.* **2012**, *187*, 142−149.
(14) Ahmed, I. M.; Gasser, M. S. Adsorption Study of Anionic Reactive Dye from Aqueous Solution to Mg−Fe−CO_3 Layered Double Hydroxide (LDH). *Appl. Surf. Sci.* **2012**, *259*, 650−656.
(15) Mustapha Bouhent, M.; Derriche, Z.; Denoyel, R.; Prevot, V.; Forano, C. Thermodynamical and Structural Insights of Orange II Adsorption by Mg_RAlNO_3 Layered Double Hydroxides. *J. Solid State Chem.* **2011**, *184*, 1016−1024.
(16) de Sá, F. P.; Cunha, B. N.; Nunes, L. M. Effect of pH on the Adsorption of Sunset Yellow FCF Food Dye into a Layered Double Hydroxide (CaAl−LDH−NO_3). *Chem. Eng. J.* **2013**, *215-216*, 122−127.
(17) Lin, Y.; Fang, Q.; Chen, B. Metal Composition of Layered Double Hydroxides (LDHs) Regulating ClO^-_4 Adsorption to Calcined LDHs via the Memory Effect and Hydrogen Bonding. *J. Environ. Sci.* **2014**, *26*, 493−501.
(18) Wu, H.; Gao, H.; Yang, Q.; Zhang, H.; Wang, D.; Zhang, W.; Yang, X. Removal of typical organic contaminants with a recyclable calcined chitosan-supported layered double hydroxide adsorbent: Kinetics and equilibrium isotherms. *J. Chem. Eng. Data* **2017**, *63*, 159−168.
(19) Chowdhury, P. R.; Bhattacharyya, K. G. Ni/Co/Ti layered double hydroxide for highly efficient photocatalytic degradation of Rhodamine B and Acid Red G: a comparative study. *Photochem. Photobiol. Sci.* **2017**, *16*, 835−839.
(20) Wang, G.; Li, Y.; Jiang, B.; Pan, K.; Fan, N.; Feng, Q.; Chen, Y.; Tian, C. In situ synthesis and photoluminescence of Eu^{3+} doped Y $(OH)_3$@ β-$NaYF_4$ core−shell nanotubes. *Chem. Commun.* **2011**, *47*, 8019.
(21) Wang, Q.; Wang, X.; Shi, C. LDH Nanoflower Lantern Derived from ZIF-67 and Its Application for Adsorptive Removal of Organics from Water. *Ind. Eng. Chem. Res.* **2018**, *57*, 12478−12484.
(22) Ai, L.; Zhang, C.; Meng, L. Adsorption of methyl orange from aqueous solution on hydrothermal synthesized Mg-Al layered double hydroxide. *J. Chem. Eng. Data* **2011**, *56*, 4217−4225.
(23) Langmuir, I. The adsorption of gases on plane surfaces of glass, mica and platinum. *J. Am. Chem. Soc.* **1918**, *40*, 1361−1403.
(24) Li, J.; Zhang, N.; Ng, D. H. L. Synthesis of a 3D hierarchical structure of γ-AlO (OH)/Mg−Al-LDH/C and its performance in organic dyes and antibiotics adsorption. *J. Mater. Chem.* **2015**, *3*, 21106−21115.
(25) Annadurai, G.; Juang, R.-S.; Lee, D.-J. Use of cellulose-based wastes for adsorption of dyes from aqueous solutions. *J. Hazard. Mater.* **2002**, *92*, 263−274.
(26) Mittal, A.; Malviya, A.; Kaur, D.; Mittal, J.; Kurup, L. Studies on the adsorption kinetics and isotherms for the removal and recovery of methyl orange from wastewaters using waste materials. *J. Hazard. Mater.* **2007**, *148*, 229−240.
(27) Liu, X.; Zhang, J.; Guo, X.; Wu, S.; Wang, S. Porous alpha-Fe_2O_3 decorated by Au nanoparticles and their enhanced sensor performance. *Nanotechnology* **2010**, *21*, No. 095501.
(28) Hu, Q.; Xu, Z.; Qiao, S.; Haghseresht, F.; Wilson, M.; Lu, G. Q. A novel color removal adsorbent from heterocoagulation of cationic and anionic clays. *J. Colloid Interface Sci.* **2007**, *308*, 191−199.
(29) Asouhidou, D. D.; Triantafyllidis, K. S.; Lazaridis, N. K.; Matis, K. A. Adsorption of reactive dyes from aqueous solutions by layered double hydroxides. *J. Chem. Technol. Biotechnol.* **2012**, *87*, 575−582.
(30) Zhang, Y. X.; Hao, X. D.; Kuang, M.; Zhao, H.; Wen, Z. Q. Preparation, characterization and dye adsorption of Au nanoparticles/ZnAl layered double oxides nanocomposites. *Appl. Surf. Sci.* **2013**, *283*, 505−512.
(31) Yan, Z.; Zhu, B.; Yu, J.; Xu, Z. Effect of calcination on adsorption performance of Mg-Al layered double hydroxide prepared by a water-in-oil microemulsion method. *RSC Adv.* **2016**, *6*, 50128−50137.
(32) Darmograi, G.; Prelot, B.; Layrac, G.; Tichit, D.; Martin-Gassin, G.; Salles, F.; Zajac, J. Study of adsorption and intercalation of orange-type dyes into Mg-Al layered double hydroxide. *J. Phys. Chem. C* **2015**, *119*, 23388−23397.
(33) Fahel, J.; Kim, S.; Durand, P.; André, E.; Carteret, C. Enhanced catalytic oxidation ability of ternary layered double hydroxides for organic pollutants degradation. *Dalton Trans.* **2016**, *45*, 8224−8235.
(34) Marçal, L.; de Faria, E. H.; Saltarelli, M.; Calefi, P. S.; Nassar, E. J.; Ciuffi, K. J.; Trujillano, R.; Vicente, M. A.; Korili, S. A.; Gil, A. Amine-functionalized titanosilicates prepared by the sol-gel process as adsorbents of the azo-dye Orange II. *Ind. Eng. Chem. Res.* **2011**, *50*, 239−246.
(35) He, C.; Hu, X. Anionic dye adsorption on chemically modified ordered mesoporous carbons. *Ind. Eng. Chem. Res.* **2011**, *50*, 14070−14083.
(36) Zhang, L.; Chen, L.; Liu, X.; Zhang, W. Effective removal of azo-dye orange II from aqueous solution by zirconium-based chitosan microcomposite adsorbent. *RSC Adv.* **2015**, *5*, 93840−93849.
(37) Géraud, E.; Bouhent, M.; Derriche, Z.; Leroux, F.; Prévot, V.; Forano, C. Texture effect of layered double hydroxides on chemisorption of Orange II. *J. Phys. Chem. Solids* **2007**, *68*, 818−823.
(38) Mandal, S.; Kalaivanan, S.; Mandal, A. B. Polyethylene Glycol-Modified Layered Double Hydroxides: Synthesis, Characterization, and Study on Adsorption Characteristics for Removal of Acid Orange II from Aqueous Solution. *ACS Omega* **2019**, *4*, 3745−3754.
(39) Prado, N.; Ochoa, J.; Amrane, A. Biodegradation and biosorption of tetracycline and tylosin antibiotics in activated sludge system. *Process Biochem.* **2009**, *44*, 1302−1306.
(40) Figueroa, R. A.; Leonard, A.; MacKay, A. A. Modeling tetracycline antibiotic sorption to clays. *Environ. Sci. Technol.* **2004**, *38*, 476−483.
(41) Chang, P.-H.; Li, Z.; Yu, T.-L.; Munkhbayer, S.; Kuo, T.-H.; Hung, Y.-C.; Jean, J.-S.; Lin, K.-H. Sorptive removal of tetracycline from water by palygorskite. *J. Hazard. Mater.* **2009**, *165*, 148−155.

https://dx.doi.org/10.1021/acsomega.9b03785
ACS Omega 2020, 5, 2368−2377

(42) Chang, P.-H.; Li, Z.; Jiang, W.-T.; Jean, J.-S. Adsorption and intercalation of tetracycline by swelling clay minerals. *Appl. Clay Sci.* **2009**, *46*, 27−36.
(43) Rathee, G.; Awasthi, A.; Sood, D.; Tomar, R.; Tomar, V.; Chandra, R. A new biocompatible ternary Layered Double Hydroxide Adsorbent for ultrafast removal of anionic organic dyes. *Sci. Rep.* **2019**, *9*, 16225.

https://dx.doi.org/10.1021/acsomega.9b03785
ACS Omega 2020, 5, 2368−2377